The Structure of an Integral Membrane Peptide: A Deuterium NMR Study of Gramicidin

R. Scott Prosser, Steven I. Daleman, and James H. Davis
Department of Physics, University of Guelph, Guelph, Ontario, Canada, N1G 2W1

ABSTRACT Solid state deuterium NMR was employed on oriented multilamellar dispersions consisting of 1,2-dilauryl-*sn*-glycero-3-phosphatidylcholine and deuterium (^{2}H) exchange-labeled gramicidin D, at a lipid to protein molar ratio (L/P) of 15:1, in order to study the dynamic structure of the channel conformation of gramicidin in a liquid crystalline phase. The corresponding spectra were used to discriminate between several structural models for the channel structure of gramicidin (based on the left- and right-handed $\beta_{LD}^{6.3}$ helix) and other models based on a structure obtained from high resolution NMR. The oriented spectrum is complicated by the fact that many of the doublets, corresponding to the 20 exchangeable sites, partially overlap. Furthermore, the asymmetry parameter, η, of the electric field gradient tensor of the amide deuterons is large ($\approx$0.2) and many of the amide groups are involved in hydrogen bonding, which is known to affect the quadrupole coupling constant. In order to account for these complications in simulating the spectra in the fast motional regime, an ab initio program called Gaussian90 was employed, which permitted us to calculate, by quantum mechanical means, the complete electric field gradient tensor for each residue in gramicidin (using two structural models). Our results indicated that the left-handed helical models were inconsistent with our observed spectra, whereas a model based on the high-resolution structure derived by Arseniev and coworkers, but relaxed by a simple energy minimization procedure, was consistent with our observed spectra. The molecular order parameter was then estimated from the motional narrowing assuming the relaxed (right-handed) Arseniev structure. Our resultant order parameter of S_{zz} = 0.91 translates into an rms angle of 14°, formed by the helix axis and the local bilayer normal.

The strong resemblance between our spectra (and also those reported for gramicidin in 1,2-dipalmitoyl-*sn*-glycero-3-phosphatidylcholine (DPPC) multilayers) and the spectra of the same peptide incorporated in a lyotropic nematic phase, suggests that the lyotropic nematic phase simulates the local environment of the lipid bilayer.

INTRODUCTION

Gramicidin A (GA) is a pentadecapeptide consisting of 15 alternating L- and D-amino acids (Sarges and Witkop, 1965) and has the following chemical formula: HCO-L-Val_1-Gly_2-L-Ala_3-D-Leu_4-L-Ala_5-D-Val_6-L-Val_7-D-Val_8-L-Trp_9-D-Leu_{10}-L-Trp_{11}-D-Leu_{12}-L-Trp_{13}-D-Leu_{14}-L-Trp_{15}-$NH(CH_2)_2OH$. The natural mixture of gramicidin, which we will refer to as GD, is obtained from *Bacillus brevis*, and contains 5–20% L-Ile in place of L-Val_1, 9% L-Phe_{11} (in place of L-Trp_{11}), and 19% L-Tyr_{11} (in place of L-Trp_{11}) (Sarges and Witkop, 1965). Pure GD can be isolated in gram quantities (Stankovic et al., 1990), or GA may be obtained with high yields, by solid-phase peptide synthesis (Fields et al., 1989). Consequently, this peptide has served as a useful model in the study of lipid/protein interactions and ion conductance (for a recent review see Killian (1992)). The molecule is also known to adopt very distinct conformations depending on its environment (Bystrov and Arseniev, 1988; Wallace, 1992; Lograsso et al., 1988; Morrow et al., 1991; Cox et al., 1992; Greathouse and Koeppe, 1992). We will concentrate on the structural properties of gramicidin A in its channel conformation (Venkatachalam and Urry, 1983) based on the application of solid state deuterium (^{2}H) NMR spectroscopy to the exchange-labeled peptide.

The structural and dynamic properties of membranous proteins are fundamentally connected with their function. Although many membranous proteins can be sequenced, expressed in milligram quantities, and functionally reconstituted into a membrane, their high resolution, three-dimensional structures are in general difficult to obtain. It is sometimes possible to incorporate membrane peptides or proteins into detergent micelles in order to obtain sufficient motional averaging for high resolution ^{1}H NMR (See for example the work of Arseniev et al. on gramicidin A (Arseniev et al., 1985, 1986) and the work of others on larger membrane proteins (Wüthrich, 1986)). X-ray diffraction studies of three-dimensional membrane protein crystals have yielded high resolution structures of the photosynthetic reaction center of *Rhodopseudomonas viridis* (Deisenhofer and Michel, 1989), although in general it has proven to be very difficult to produce three-dimensional crystals of membrane proteins (Gennis, 1989). Recently, a gramicidin/phospholipid complex has been crystallized and studied by x-ray diffraction (Wallace, 1991, 1992). Although the structure of the peptide/lipid co-crystal has not yet been solved, the diffraction data is consistent with a channel-like helical dimer containing 6.3 residues per turn (Wallace, 1991, 1992). The preparation of two-dimensional crystals of a given membrane peptide for purposes of cryoelectron microscopy and three-dimensional image reconstruction (Henderson et al., 1990) is sometimes possible. Compared to the growing of two- or three-dimensional crystals, it is sometimes easier to

Received for publication 15 June 1993 and in final form 16 February 1994.
Address reprint requests to James H. Davis, Department of Physics, University of Guelph, Guelph, Ontario, Canada N1G 2W1.
Present address (R. S. P.): Institut für Physikalische Chemie, der Universität Stuttgart, Pfaffenwaldring 55, D-70569 Stuttgart, Germany

0006-3495/94/05/1415/14 $2.00

obtain uniaxially oriented membrane proteins, in which case solid-state NMR can in principal reveal the complete high resolution protein structure in addition to information on dynamics (Opella et al., 1987; Opella and Taylor, 1989). However, this technique requires a massive investment of time to accomplish the isotopic labeling and to perform the experiments. Using ^{14}N, ^{15}N, and ^{13}C solid state NMR, Cross and coworkers are attempting to determine the complete backbone structure of the gramicidin channel, using isotopically labeled GA in oriented phospholipid dispersions (Ketchem and Cross, personal communication; Lograsso et al., 1988; Moll and Cross, 1990). Instead of specifically labeling the peptide of interest, we have chosen to study ^2H exchange-labeled GD, incorporated into oriented 1,2-dilauryl-*sn*-glycero-3-phosphatidylcholine (DLPC) multilayers. In this case, there are at least 20 distinct labels, leading to a complicated oriented spectrum. Such a spectrum contains a wealth of structural information. Rather than attempting to assign each peak, our approach has been to use the exchange-labeled spectra to "fingerprint" the peptide and assess existing structural models by comparing their corresponding predicted exchange-labeled spectra.

Deuterium NMR is particularly suited to the study of dynamic structure in partially ordered systems. At high fields ($B_0 > 1T$) the magnitude of the electric quadrupole interaction of the $I = 1$ ^2H nucleus is sufficiently small, relative to the Zeeman interaction, that a simple first-order perturbation treatment may be used. The strengths of the magnetic dipole-dipole and chemical shift interactions are such that the quadrupolar interaction typically dominates both the observed spectra and the spin relaxation. Moreover, the principal component of the quadrupole coupling tensor generally lies along or nearly along the C—^2H, O—^2H, or N—^2H bond (Vold and Vold, 1991). Although the electric field gradient (EFG) asymmetry parameter (η) can be as high as 0.2 in an N—^2H bond, the splittings in the fast motionally symmetric regime are independent of η. Under such ideal circumstances, the experimentally obtained quadrupolar splitting yields the average orientational order $S = (1/2)(\overline{3\cos^2\theta - 1})$, where θ defines the angle between the above mentioned bond and the symmetry axis. Thus, it is not unreasonable to expect to be able to accurately predict the experimental spectrum given a structural model (i.e., the "fingerprint" is entirely reproducible from a reliable three-dimensional picture).

Although solid-state NMR may be used to determine structure in a model-independent way, in a more practical sense the spectra from even a few well chosen labels can be used to compare competing structural models (Prosser et al., 1991). By careful lineshape analysis of oriented multilayers of isotopically labeled gramicidin, it is also possible to address more sophisticated structural problems. For example, Killian et al. have examined ^2H NMR lineshapes from oriented Val_1 (d_8) GA to interpret average side chain orientations in terms of channel-stabilizing hydrophobic interactions (Killian et al., 1992). It is important to recognize that solid state NMR spectra reflect both a time- and ensemble-averaged microscopic picture. Thus, structural properties like supramolecular organization, or dynamic properties such as dimerization rates (depending on their time scale), may be entirely missed even by the most careful NMR experiments. Single channel conductance measurements (which permit the study of single molecular events) on GA analogues indicate that the elementary conductance unit of a gramicidin channel is a dimer, and that dimerization may be stabilized by lateral aggregation (possibly tetramers). However, recent x-ray scattering with the momentum transfer confined in the plane of the membrane suggests the GA channels are randomly distributed in the membrane plane (He et al., 1993). On an even higher level of organization, the phase behavior of gramicidin-phosphatidylcholine mixtures has also been studied by DSC and ^2H NMR difference spectroscopy (Morrow and Davis, 1988).

Progress is being made on all fronts in the investigation of the three-dimensional structure, dynamics, function, organization, and phase behavior of the channel conformation of the membrane peptide, gramicidin A. Our strategy has been to employ ^2H NMR on oriented ^2H exchange labeled GD in order to gather as much orientational information on the peptide as possible. Although assignment of all the doublets is not possible without additional double resonance schemes, we will show that the three-dimensional structural models of the peptide can be critically compared by predicting their corresponding ^2H exchange-labeled fast motional limit spectra with the observed spectra. We will also show that some of the complications associated with predicting EFG tensors for hydrogen-bonded deuterons can be treated effectively by resorting to ab initio quantum mechanical calculations. In addition, we will discuss calculations on the molecular order parameter based on the observed motional narrowing.

MATERIALS AND METHODS

Preparation of oriented samples

In order to obtain optimally aligned oriented samples we elected to use DLPC as the lipid host. The phase behavior and structure of this lipid have recently been studied (Morrow and Davis, 1987; Katsaras et al., 1994). The following procedure was used to prepare multilayers of ^2H exchange-labeled DLPC/GD, oriented on glass plates:

1. *Plate cutting*—0.1-mm thick glass coverslip plates (Fisher Scientific, Toronto) were cut in three sizes: (0.83 × 2.45, 0.68 × 2.45, and 0.44 × 2.45 cm).
2. *Preparation of ^2H exchange-labeled GD*—About 0.75 g of GD (Sigma Chemicals, St. Louis, MO) was dissolved in 50 ml of $C^1H_3O^2H$ (MeOD) (MSD Isotopes, Dorval, Quebec) and left at room temperature for 1 month to allow for nearly complete exchange of all labile hydrogen.
3. *Plate cleaning*—The precut plates were thoroughly rinsed in ethanol, acetone, redistilled water, ethanol, and finally methanol/dichloromethane (1:3 by volume), before being vacuum-dried.
4. *Preparation of peptide/lipid mixture*—Roughly 250 mg of DLPC and ^2H exchange-labeled GD (15:1 molar ratio) was completely dissolved in 30 ml of MeOD, then left at 40°C for 90 min. The bulk of the solvent was removed by rotary evaporation, and the remainder was removed by drying under vacuum overnight. Exactly 163 mg of dry sample was transferred to a 4-ml test tube. 2850 μl of MeOD/^2H_2O (9:1 by volume) was added to the test tube, such that 2 mg of sample (dry) would be applied per cm^2 plate area using a solvent concentration of 35 μl/cm^2 (for optimal wetting and spreading of the sample on the plates). The mixture was

gently stirred until it was completely dissolved. A small amount of Hepes buffer salt was also added to the solvent such that a concentration of roughly 0.016 M buffer would be obtained under maximum hydration.

5. *Application of sample to plates*—The sample was next pipetted onto the dry glass plates and allowed to air dry (for 30 min). The plates were dried in a vacuum overnight and stacked inside the NMR tube. In all we were able to stack 11 large plates, 12 medium sized plates (six on top and six underneath the large plates), and 11 small plates plus a spacer, making a total of 35 plates in all.
6. *Hydrating and annealing*—The sample was placed in a warm (60°C) hydrating environment (^2H_2O) overnight, after which it was annealed for 3 days by alternately hydrating at 50°C for 21 h and drying at 50°C for 3 h. Lastly, the sample was placed in a closed ^2H_2O environment at room temperature for several more days.

Our plates held about 120 mg of sample, of which 21 mg was GD, corresponding to 208 μM of deuterium.

Verification of the channel conformation by circular dichroism

Gramicidin is known to adopt both channel and nonchannel conformations in the membrane. Fortunately, the circular dichroism (CD) signatures of each conformation are completely different and well documented (Lograsso et al., 1988; Morrow et al., 1991; Bano et al., 1991; Killian et al., 1988). We therefore employed this spectroscopic technique to confirm that the peptide had adopted the channel conformation in DLPC, using the sample preparation method described above. The CD spectra for gramicidin/DLPC (1:15 molar ratio) were recorded with a J-600 spectropolarimeter (Japan Spectroscopic Co., Tokyo) (data not shown). The sample preparation regime for the CD measurements was identical to the preparation scheme for the NMR experiments, except that the sample was ultimately diluted and centrifuged (to remove light-scattering aggregates (Lograsso et al., 1988)).

^2H NMR experiments

Our study of the dynamic structure of an intramembranous peptide involved quadrupole echo (Davis et al., 1976) inversion-recovery, and modified Jeener-Broekaert pulse sequences, the details of which have been documented elsewhere (Davis, 1983; Vold and Vold, 1991). Each of these pulse sequences was preceded by a "soft" π-pulse designed to selectively eliminate the water signal (or any spectral component very near to the center frequency). The quadrupole echo (QE) and inversion-recovery (IR) pulse sequences may be described as follows: QE: $(\pi/2)_x - \tau_1 - (\pi/2)_y$; IR: $(\pi)_x - \tau_2 - (\pi/2)_x - \tau_1 - (\pi/2)_y$

The particular phase cycling schemes for the above sequences may be found elsewhere (Vold and Vold, 1991). Typically, between 40,000 and 120,000 scans were accumulated, with a refocusing time (τ_1) equal to 35 μs, and a repetition time of 0.35 s. The water saturation pulse was typically 150 μs, with a delay time of 0.1 s before the first hard pulse. The dwell time was set to 1 or 2 μs (depending on the spectral width) and the analogue filters to 350 kHz. The duration of a (π) pulse was typically 7.1 μs using an 8-turn solenoid coil with an inner diameter of 11 mm and a length of 20 mm.

Note that the rather long pulse lengths and very large splittings create severe spectral distortion, especially for the spectra obtained from plate orientations of $\theta_{or} = 0°$ where the outermost splittings were as high as 266 kHz. Bloom et al. have described the spectral distortion effects due to finite pulse widths (Bloom et al., 1980). For a single π pulse, of length 7.1 μs, a doublet whose quadrupolar splitting is 266 kHz will be reduced to about 0.4 times what its value would be for an infinitely short pulse; for a single $\pi/2$ pulse (3.55 μs), the distortion of the outer doublet for the 90° orientation is only 0.9. Such losses in intensity are necessary evils when working with large oriented samples. However, to reduce this distortion somewhat, a Levitt-Suter-Ernst composite $\pi/2$ pulse (Heaton, et al., 1988) equal to $(3\pi/4)_x(\pi/2)_{-x}(\pi/4)_x$ was used in the QE sequence, and a composite inversion pulse equal to $(\pi/2)_x(\pi/2)_y(\pi/2)_x$ was used in the IR sequence. All experiments were performed in an 8.5T magnet corresponding to a ^2H Larmor frequency $\nu_0 = 55.265$ MHz.

Analysis of FIDs

FIDs, obtained in quadrature from one of the above pulse sequences, were analyzed with software adapted from that of Dennis Hare (Hare Research, Woodinville, WA). An autophase correct algorithm adjusted the complex FID such that the real part of the FID was a pure absorption signal. The contribution to the echo due to the residual water signal was removed by a polynomial fit and subtraction of the slowly varying component. The last few points of the FID were used to automatically adjust the baseline offset to zero. To obtain an undistorted spectrum and improve on the S/N the raw data set was contracted (Prosser et al., 1991; Davis, 1983) and multiplied by an exponential (250-Hz broadening) before being Fourier transformed.

Simulation of spectra in the fast motional regime

In the fast axially symmetric motional regime the ^2H exchange-labeled spectra can be simulated using only the quadrupole coupling constant (e^2qQ/h), the Euler angle (θ_D) (whose magnitude equals the angle between a particular N—^2H bond and the molecular diffusion axis) and T_{2E}, for each label. In this "zeroth order" approximation we ignore both the variation in the quadrupole coupling constant due to hydrogen bonding and the asymmetry parameter (η) associated with the EFG tensor. In this case, for each labeled position, θ_D can be extracted directly from the three-dimensional model, and T_{2E} can be approximated from a phenomenological expression. Higher levels of approximation were also attempted. We accounted for the variation in the quadrupole coupling constants by employing a phenomenological equation in which e^2qQ/h decreased proportionally with the inverse cube of the distance between the ^2H and the adjacent O atom (Hunt and MacKay, 1974, 1976). At an even higher level of approximation, the complete EFG tensor in the molecular diffusion tensor system may be calculated from the lowest energy electronic molecular orbital using an ab initio program called Gaussian90 (Frisch et al., 1990). Such a calculation (which must be done for each residue in each molecular model) in principle accounts for the influence of hydrogen bonding on e^2qQ/h and yields the Euler angles $\{\phi_D, \theta_D, \text{and } \psi_D\}$ which transform the EFG tensor from the EFG principle axis system (PAS) to the molecular diffusion tensor system (Meier et al., 1986). This calculation was performed using the experimentally derived Arseniev model (Arseniev et al., 1985, 1986) and a model which used the Arseniev structure as a starting conformation in an energy minimization calculation (Killian et al., 1992). The Gaussian90 calculations were usually performed on a Silicon Graphics 4D/380VGX workstation using an STO-3G* basis set for the molecular orbitals (Frisch et al., 1990). Higher basis sets such as the MP2/6-31G were employed using a Silicon Graphics 4D/310S workstation. In all cases, the structural models were first oriented along the mathematically derived helix axis by a least squares fit of the backbone atoms to the surface of a cylinder (Åqvist, 1986). Thus, the spectrum could be completely simulated from the three-dimensional molecular model.

RESULTS AND DISCUSSION

Characterizing the lipid/peptide system using chain perdeuterated lipids

We began this study of dynamic structure by characterizing the lipid/peptide system using ^2H NMR on chain perdeuterated DLPC. Fig. 1 shows two oriented ($\theta_{or} = 0°$) quadrupole echo spectra of DLPC-d_{46} alone (*a*) and DLPC-d_{46} with GD (L/P = 15:1) (*b*), at 35°C. The addition of gramicidin results in a significant broadening of the oriented spectra and a slight reduction in the splitting of the outermost doublets. This result may be compared with the findings of Rice and Oldfield (1979) who employed ^2H NMR to study the interaction between GD, and DMPC specifically labeled with deuterium at one of positions 2, 3, 4, 6, 8, 10, 12, or 14 on the *sn*-2 chain. In this study, it was found that at L/P $\geq$ 15:1, the quadrupolar

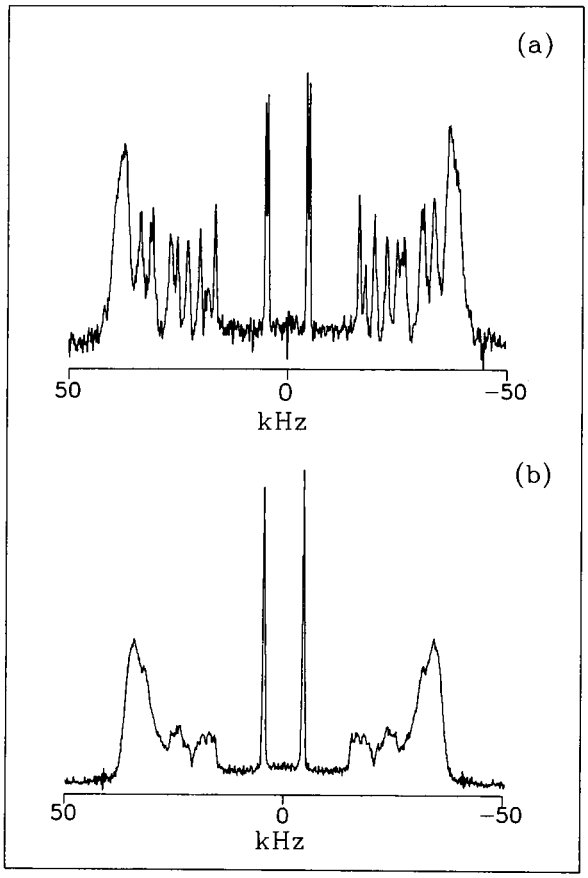

FIGURE 1 ^{2}H NMR quadrupole-echo spectra of DLPC-d_{46} (*a*) and GD/DLPC-d_{46} (*b*), at 35°C, oriented at $\theta_{or} = 0°$. These spectra were each obtained from a single glass plate (3000 scans), using a 3.0 μs $\pi/2$ pulse length, 40 μs τ, and 0.5-s repetition time. The distribution of sample on the glass plates was 3 and 2 mg/cm^2 for *a* and b, respectively.

splittings ($\Delta\nu_Q$) of the labels increased linearly with gramicidin concentration to a value ~30% greater than that of the pure lipid. Between L/P values of 15:1 and 4:1, the splittings then decreased slowly. The authors suggested that the hydrocarbon chains of the lipids adjacent to the peptide are disordered; conformational transitions therefore occur at a slower rate, accounting for the observation of rigid lattice ESR spectra (Rice and Oldfield, 1979). However, $\Delta\nu_Q$ decreases since these fluctuations are still fast on the ^{2}H NMR time scale (Rice and Oldfield, 1979). At low gramicidin concentrations the lipid spends most of its time far from the peptide. The increase in splittings as peptide concentration is raised is a reflection of the increased ordering of the bulk lipid phase, perhaps accompanied by an increase in bilayer thickness. At high gramicidin concentrations the peptide disrupts the lipid chain packing (Rice and Oldfield, 1979). Rice and Oldfield also observed significant broadening of the methylene lineshapes upon the addition of even small amounts of gramicidin, which they suggested was due to some motional process with a correlation time on the order of the inverse of the quadrupole coupling constant. We now know that, in the liquid crystalline phase of DMPC, whole body and internal lipid motions are orders of magnitude faster than this characteristic time scale (Mayer et al., 1988) and that T_{1Z}, which reflects these faster lipid motions, is changed very little by the addition of peptide (Prosser et al., 1992). We are therefore left with three possibilities:

1. The exchange rate between the bulk lipid and the surrounding lipid layer occurs on a time scale comparable to the inverse of the quadrupole coupling constant.
2. The addition of gramicidin alters the physical properties of the membrane such that collective motions become T_{2E}-effective (Prosser, et al., 1992).
3. Gramicidin experiences some slow motions ($\approx 10^{-6}$ s). These motions in turn influence the lipid broadening.

Note that in Fig. 1 *a* the inequivalence in the methyl deuterons can clearly be seen by the two distinct methyl splittings. Morrow (1990) notes that for DMPC multilayers above 13°C containing 1, 2, and 4 mol % gramicidin, T_{2E} decreases with peptide added, except for the methyl deuterons which show the opposite dependence. As can be seen in Fig. 1 *b*, the addition of gramicidin removes the inequivalence in the *sn*-1 and *sn*-2 methyl groups. Davis (1993) has noted that an increase in orientational order, as caused by the addition of cholesterol for example, results in an increase in chain inequivalence.

^{2}H NMR spectroscopy of exchange-labeled gramicidin D

Basic treatment in the fast motionally symmetric regime

Having characterized the lipid-peptide system by circular dichroism and ^{2}H NMR from the perspective of the lipid, we proceeded to investigate the labeled peptide in oriented DLPC multilayers. In this section we will introduce the formalism necessary to interpret ^{2}H NMR quadrupolar splittings, particularly in the fast axially symmetric motional regime. Within this formalism we will discuss the results of our work on ^{2}H exchange-labeled gramicidin D in oriented DLPC multilayers.

The quadrupolar Hamiltonian for deuterium ($\mathscr{H}_Q$) arises from the interaction between the electric quadrupole moment (eQ) and the EFG at the nucleus. In a large magnetic field (B_0), the strength of this tensorial interaction is sufficiently small that one can treat $\mathscr{H}_Q$ as a first-order perturbation on the Zeeman interaction. Using spherical tensor notation, one can then write a simple first-order expression for the quadrupolar Hamiltonian in the EFG tensor PAS (Davis, 1983). One must then employ Wigner rotation matrices to transform from the PAS system to the laboratory system. The Euler angles $\{\phi_D, \theta_D, \psi_D\}$ accomplish the transformation from the PAS (in which the z axis is generally along the N—^{2}H bond when the asymmetry parameter (η) is zero) to the diffusion tensor system (with the z axis along the helix axis (Prosser et al., 1991; Separovic et al., 1993). The Euler angle, θ defines the transformation of the EFG tensor from the diffusion tensor system to the director system (for simple diffusion around the helix axis, $\theta = 0$), where the z axis lies along the local bilayer normal (in the absence of order director fluc-

tuations, the local bilayer normal will also be normal to the glass plates). The Euler angle θ_{or} defines the final transformation into the laboratory frame (z axis along the principal magnetic field), where we may express the splitting as (Davis, 1983, 1993)[1]

$$\Delta\nu_Q = \frac{3}{4}\frac{e^2qQ}{h}(3\cos^2\theta_{or} - 1)\frac{1}{2} \cdot (3\cos^2\theta - 1)\frac{1}{2}[(3\cos^2\theta_D - 1) + \eta\cos 2\phi_D \sin^2\theta_D]. \quad (1)$$

The bars in the above equation represent either an ensemble- or time-average. For example, fast local internal motions would effectively average the EFG tensor, while wobbling of the peptide (which we presume to be uncoupled from internal motions) would lead to a time-averaged value of $(1/2)(3\cos^2\theta - 1)$. The EFG tensor is a traceless, symmetric second rank tensor, V_{ij}, which in its principal axis system consists of only two independent components: $V_{zz} = eq$ and $\eta \equiv (V_{xx} - V_{yy})/V_{zz}$ where $|V_{xx}| \leq |V_{yy}| \leq |V_{zz}|$ and $0 \leq \eta \leq 1$. If $\eta \approx 0$ (which is the case for deuterons in C—^{2}H bonds), θ_D represents the angle between the bond formed by the deuteron and its directly bonded atom, and the axis of motional averaging. For the moment we will assume that the peptide is rigid and undergoes only diffusion around its long (helix) axis. The helix axis is in turn assumed to be parallel with the local bilayer normal such that $\theta = 0$. Moreover, under the condition of fast axially symmetric motion, the rotational diffusive motions modulate ϕ_D randomly causing the second term in Eq. 1 to average to zero, so that

$$\Delta\nu_Q = \frac{3}{4}\frac{e^2qQ}{h}(3\cos^2\theta_{or} - 1)\frac{1}{2}(3\cos^2\theta_D - 1). \quad (2)$$

Gramicidin A possesses 16 amide and four indole groups which may be readily exchange-labeled. The corresponding ^{2}H NMR spectrum provides a discriminating test of a given structural model and, as we have seen, the expression for the splitting is straightforward. In this paper we will consider six models of the gramicidin channel and their corresponding ^{2}H NMR spectra. These models include left- and right-handed versions of the $\beta^{6.3}_{LD}$ helix proposed by Venkatachalam and Urry (Venkatachalam and Urry, 1983; 1984) and the *relaxed* counterparts of these models obtained by molecular dynamics simulations (MDS) for 80 ps (Chiu et al., 1990), as well as the experimentally obtained Arseniev structure (Arseniev et al., 1985) and its counterpart relaxed by an energy minimization (Killian et al., 1992). We will also pay close attention to the (spectroscopic) effects of hydrogen bonding and the non-zero asymmetry parameter, and to methods which best account for these effects in the simulated spectra.

Fig. 2 displays ^{2}H NMR spectra of exchange-labeled GD in oriented DLPC multilayers at two temperatures in the liquid-crystalline phase. The large number of resolvable doublets suggests an irregular structure. It is useful to compare our spectra with ^{2}H exchange-labeled GD in other types of lipid multilayers. The dePaked spectrum of exchange-labeled GD in DPPC (1:13 molar ratio) at 52°C, reported by Datema et al. (1986) (their Fig. 5), is remarkably similar to our oriented spectra presented in Fig. 2, although considerably lower in resolution. In both cases one can observe four principal groups of doublets. We can also compare our oriented spectra with those of Davis (1988) in which a unique liquid crystal host (potassium laurate/decanol/KCl/water) was employed. The spectrum at 46°C ($\theta_{or} = 90°$), reported by Davis (his Fig. 3), resembles the high temperature spectrum in Fig. 2 *a*, although the relative intensities of the peaks and the extent of motional narrowing are different (i.e., the T_{2E}-effective dynamic processes taking part in each of the two systems may be different). Apparently, the lyotropic nematic phase simulates the local environment of the lipid bilayer while yielding high resolution oriented spectra.

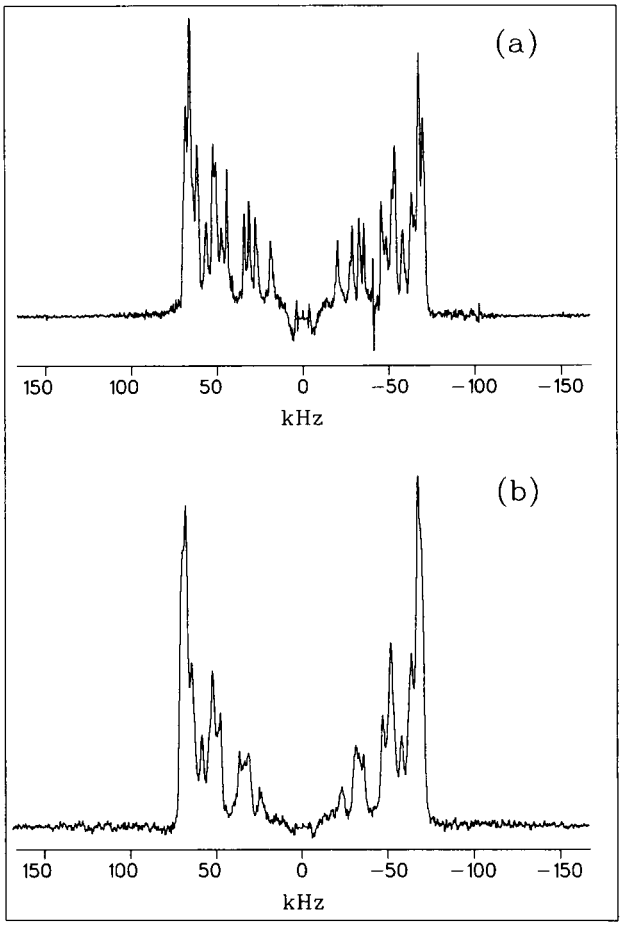

FIGURE 2 ^{2}H NMR spectra of exchange-labeled GD in oriented (θ_{or} = 90°) DLPC multilayers at 65 (*a*) and 35°C (*b*), where the lipid to peptide ratio is L/P = 15. Each spectrum is actually the sum of spectra for the four smallest tau values in a T_{1Z} relaxation experiment. The number of scans is effectively 120,000, while the 180° pulse length is 7.1 μs. As with all of our experiments on oriented GA, the inversion pulse consisted of a Levitt-Suter-Ernst composite pulse.

[1] In the above description, we have maintained a notation and Euler angle convention similar to that used by Meier et al. (1986).

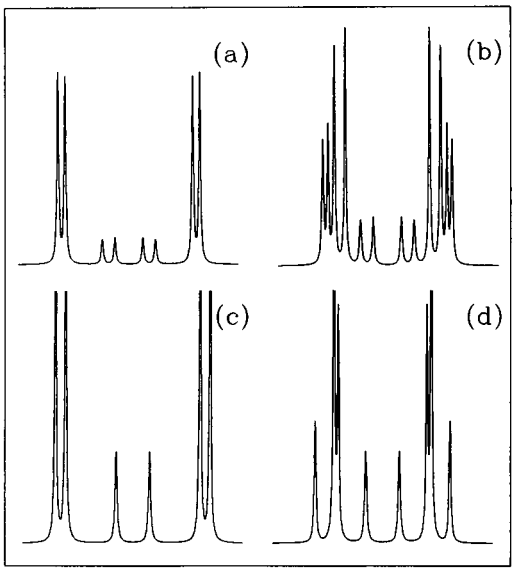

FIGURE 3 Theoretical fast motional limit ^{2}H NMR spectra of oriented exchange-labeled GD, assuming a left-handed $\beta^{6.3}_{LD}$ helix (*a* and b) and a left-handed $\beta^{6.3}_{LD}$ helix run on a molecular dynamics simulation (MDS) for 80 ps (*c* and *d*). The spectra have been calculated both with (*b* and *d*) and without (*a* and *c*) the effects of hydrogen bonding. In this case hydrogen bonding is taken into account by an empirical formula which relates the quadrupole coupling constant to the length of the hydrogen bond. Since these spectra are presumed to arise from the fast symmetric motion regime, η is effectively zero.

In the simplest approximation, the splittings in the simulated spectra may be obtained assuming a constant value for e^2qQ/h; the hydrogen bonding effects are ignored and η is approximated to be zero, in which case the splitting is completely determined by the angle formed between the N—^{2}H bond and the axis of motional averaging. Our previous work (Prosser et al., 1991) (and that of Separovic et al. (1993)) with specifically labeled GA, suggested the axis of motional averaging to be along the helix axis. In order to determine the helix axis for a finite irregular helical model, we used a program which performed a least squares fit of the backbone atom coordinates to a cylindrical surface (Åqvist, 1986). Furthermore, in simulating our spectra, we can qualitatively reproduce the experimentally observed variation of T_{2E} across the spectrum by assuming (Davis, 1979)

$$\frac{1}{T_{2E}} \propto \text{const} + (e^2qQ/h)^2(1 - S^2), \qquad (3)$$

where $S = \overline{(1/2)(3\cos^2\theta_D - 1)}$ $(= P_2(\cos\theta_D))$. Another detail is that the indole moieties typically exchange only 67% as well as the amides (Davis, 1988). Since our labeling protocol was identical to that of Davis (1988) we have incorporated the reduced indole intensities into our simulated spectra. Finally, a motional narrowing factor, which reduces all of the quadrupolar splittings in the theoretical spectrum by the same amount, can be determined such that the outermost theoretical splitting agrees with the experimentally observed value. We assume that the fast internal molecular motions and the wobble of the entire peptide that modulate θ_D and θ, respectively, are independent of each other so that

$$\overline{P_2(\cos\theta)P_2(\cos\theta_D)} = \overline{P_2(\cos\theta)}\cdot\overline{P_2(\cos\theta_D)} = S_{mol}\overline{P_2(\cos\theta_D)}, \qquad (4)$$

which permits us to estimate the molecular order parameter (S_{mol}) from the splitting (given the coupling constant and $P_2(\cos\theta_D)$).

Accounting for hydrogen bonding

At the next level of sophistication, we can account for the known hydrogen bonds using an empirical expression derived from nuclear quadrupole resonance work on deuterated amino acids at 77 K (Hunt and MacKay, 1974, 1976)

$$\frac{e^2qQ}{h} = 253\text{–}572/R^3 \quad \text{kHz}, \qquad (5)$$

where R represents the ^{2}H . . . O hydrogen bond length in angstroms. The experimental spectra of Fig. 2 may be compared with the simulated fast motional limit spectra in Figs. 3, 4, and 5, for each of the six structural models mentioned above. In this case we have separately ignored the effects of hydrogen bonding and incorporated the hydrogen bonding effects via Eq. 5. The spectra in Fig. 3 corresponding to the left-handed models bear little resemblance to the experimental spectra. The spectra in Fig. 4 corresponding to the right-handed $\beta^{6.3}_{LD}$ helix model compare favorably with the experimental spectrum, once hydrogen bond effects are accounted for. The Arseniev model (Arseniev et al., 1986) in which hydrogen bond effects have been accounted for and the *relaxed* Arseniev models (Killian et al., 1992) also give a qualitative agreement with the observed spectra (Fig. 5). If we ignore the hydrogen bonding effects, the *relaxed* Arseniev model yields a theoretical spectrum which is very close to that observed at 65°C (Fig. 5 c). Upon closer scrutiny of the right-handed models, we see that there are seven

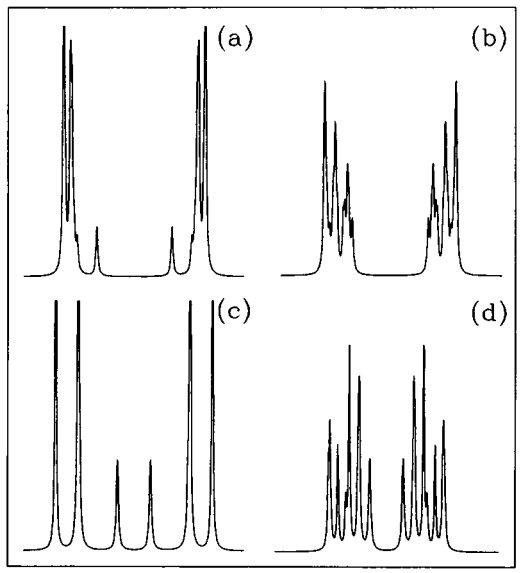

FIGURE 4 Theoretical fast motional limit ^{2}H NMR spectra of oriented exchange-labeled GD, assuming a right-handed $\beta^{6.3}_{LD}$ helix (*a* and *b*) and a right-handed $\beta^{6.3}_{LD}$ helix relaxed by MDS for 80 ps (*c* and *d*). The spectra have been calculated both with (*b* and *d*) and without (*a* and *c*) the effects of hydrogen bonding. Hydrogen bonding is taken into account by an empirical formula which relates the quadrupole coupling constant to the length of the hydrogen bond. Since these spectra are presumed to arise from the fast symmetric motion regime, η is effectively zero.

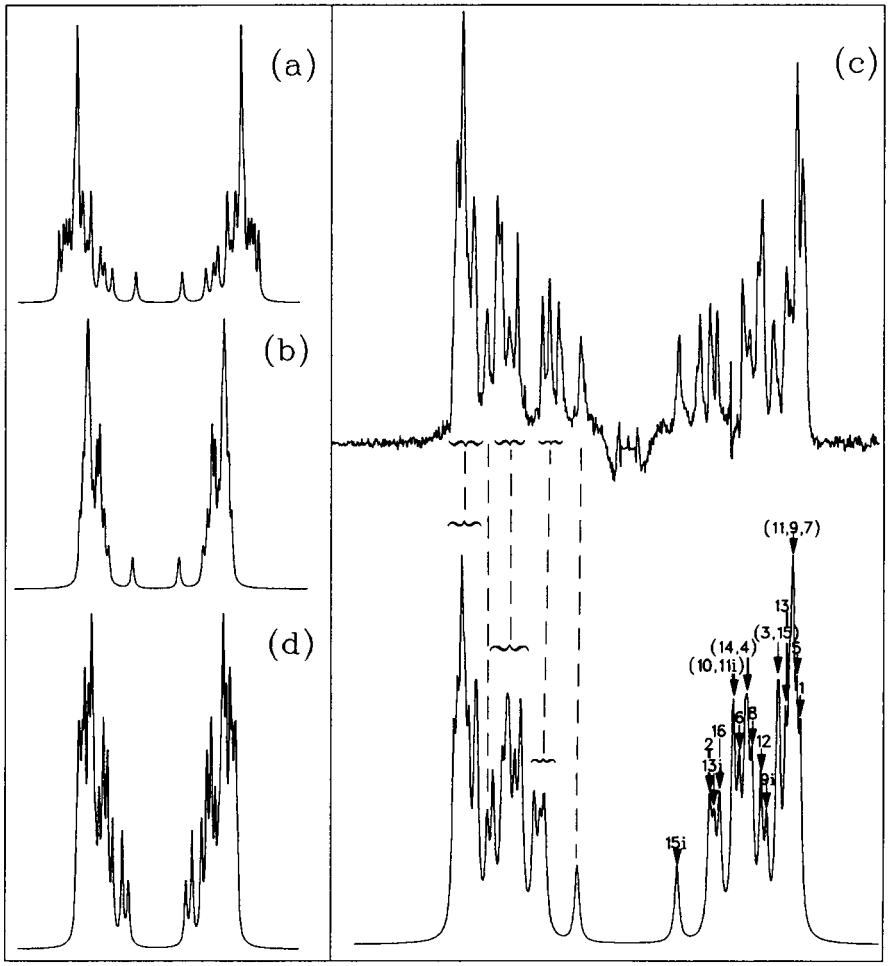

FIGURE 5 Theoretical fast motional limit ^{2}H NMR spectra of oriented exchange labeled GD, assuming the experimentally derived Arseniev structure (*a* and *b*) and a relaxed version of the Arseniev structure (*c* and *d*). The spectra have been calculated both with (*b* and *d*) and without (*a* and *c*) the effects of hydrogen bonding. In this case, hydrogen bonding is taken into account by an empirical formula which relates the quadrupole coupling constant to the length of the hydrogen bond. Since these spectra are presumed to arise from the fast symmetric motion regime, η is effectively zero. In *c*, which compares the *relaxed* Arseniev model with the experimental spectrum of Fig. 2 *a*, the peaks in the theoretical spectrum have been labeled according to the residue from which they originate. The suffix "i" after the residue number indicates the indole moiety and the number(s) assigned to a given peak indicate(s) the residue number.

N—^{2}H groups per monomer (four of which are indole moieties) which are not hydrogen bonded to other atoms within the dimer. Furthermore, six of these seven N—^{2}H groups lie in the outermost turn of the dimer which has been suggested to possess greater conformational flexibility (Smith et al., 1989). We also expect some of the deuterons from the outermost turn to be involved in hydrogen bonding to water molecules. However, without further details on internal motions and on the water molecule exchange processes associated with these outer turn labels, we cannot accurately assess the inner splittings. Although such details are beyond the scope of the models presented in this paper, Roux and Davis (B. Roux, and J. H. Davis, personal communication) are attempting to calculate the time-averaged $\overline{1/2(3\cos^2\theta_D - 1)}$ from a molecular dynamics simulation of the peptide, explicitly including the water molecules.

Using ab initio quantum mechanical calculations to determine the complete EFG tensor:

Until now, we have ignored the fact that the EFG tensor at the deuterium nucleus in an N—^{2}H bond is not axially symmetric. Deuterium NMR lineshape simulations of ^{2}H exchange-labeled GD (Datema et al., 1986) and quadrupole resonance studies of deuterated amino acids (Hunt and MacKay, 1974, 1976) both suggest that typical deuteron asymmetry parameters might be as high as 0.17. In this case, we expect that θ_D (which equals the second Euler angle in the transformation of the EFG tensor from its PAS to the molecular diffusion tensor system) would no longer equal the angle formed between the N—^{2}H bond and the helix axis (molecular diffusion *z* axis). Knowledge of this tensor (for each exchangeable deuteron in GD) yields the parameters necessary to describe the spectrum in the fast motional limit (i.e., e^2qQ/h, η, ϕ_D, θ_D, and ψ_D). The EFG tensor in the diffusion tensor system can be determined from the lowest energy electronic molecular orbital at the nucleus of interest. Although computationally intensive, it is possible to calculate an approximation to this orbital using an ab initio quantum mechanical program called Gaussian90 (Frisch et al., 1990). By using such quantum computational techniques one can also account for the influence of hydrogen bonding on the EFG tensor. The above mentioned parameters may then be used in a complete NMR relaxation analysis, as will be discussed in a subsequent paper on peptide dynamics (Prosser and Davis, 1994).

The difficulties in calculating the many electron wave-functions can be appreciated by considering a two-electron atom. In the spirit of the self-consistent field (SCF) method, we imagine that each electron moves in a mean field due to the shielded nucleus and the remaining electron (Hinchliffe, 1987; Simons, 1991; Szabo and Ostlund, 1982). Electron 2 thus experiences a potential (Hinchliffe, 1987) due to both the nucleus of charge Z at a distance r_2 and to an effective charge distribution, $-e\psi_A^2$, from electron 1. Via a one-electron-like energy eigenvalue equation which incorporates electron spin and antisymmetry effects (Hinchliffe, 1987), the wave function of the second electron (ψ_B) may be determined. Obviously, ψ_A must be known to determine ψ_B. Thus, an iterative process is involved in order to calculate both wave functions, while minimizing the energy eigenvalues under the constraint that the orbitals remain orthogonal (Hinchliffe, 1987; Simons, 1991; Szabo and Ostlund, 1982). In constructing molecular electronic orbitals from atomic orbitals, the basis orbitals commonly used have two different forms: Slater-type orbitals (STOs), which have an exponential term, $e^{-\zeta r}$, and Gaussian-type orbitals (GTOs), which have a Gaussian term, $e^{-\alpha r^2}$. Since the multicenter integral calculations can not be efficiently performed with Slater-type orbitals, three or more Gaussian-type orbitals are usually combined to represent a particular Slater orbital. The bulk of our

calculations were performed, using an STO-3G* basis set, in which three GTOs were used to approximate an STO, although for one of the smaller molecular fragments, we also employed a 6-31G* basis set (six GTOs per STO). The * in the basis set notation refers to the use of polarization functions in the basis set, which give additional flexibility to the molecular orbital basis set (Simons, 1991). There also exist numerical methods for accounting for electron correlation beyond the SCF approach. We tried such an approach on one of our molecular fragments using six GTOs per STO (i.e., an MP2/6-31G basis) (Prosser, 1992).

The strategy in implementing Gaussian90 is simple: since the EFG tensor is a short range quantity, it should be possible to extract a group of 30 or 40 atoms, centered around a given N—^{2}H bond, (including the hydrogen-bonded fragment) to approximate the many electron wave function (and hence the EFG tensor) at the nucleus of interest. The only remaining problem is how to close off the given molecular fragment without completely altering the wave function. Our solution was to create a break between two singly bonded C atoms, replace each endpoint C atom (attached to the "inner" C via an sp^3 bond) with an H atom, and place the H atom at an appropriate distance from the inner C. The molecular fragments used in our calculations are illustrated in Fig. 6, where the hydrogen-bonded fragments and boundary atoms have been included. Ultimately, we obtain an EFG tensor in the molecular diffusion tensor frame, from the quantum calculations. At this point, we diagonalized the given EFG tensor and determined the Euler angles necessary to transform from the PAS system to the molecular diffusion tensor system (Prosser, 1992).

Having computed the EFG tensor (and thus e^2qQ/h, η, ϕ_D, θ_D, and ψ_D) in the molecular diffusion frame, for each labeled position and for both the Arseniev model (Arseniev et al., 1985, 1986) and the "relaxed" Arseniev model (Killian et al., 1992), we could then construct simulated spectra for the two models. Before doing this we compared our theoretical EFG tensors with results from quadrupole resonance studies of amino acid residues (Hunt and MacKay, 1974, 1976) and a ^{2}H NMR lineshape analysis of exchange-labeled gramicidin D in unoriented DPPC multilayers (Datema et al., 1986). Our first observation was that the quadrupole coupling constants derived from Gaussian90 were all about 10% higher than those typically found from NMR (Datema et al., 1986; Davis, 1988) and quadrupole resonance studies (Hunt and MacKay, 1974, 1976). Work by Ragle et al. (1974) suggests that the field gradient in the neighborhood of the deuteron may be significantly affected by the polarization of the N—^{2}H bond due to medium or solvent effects. This is consistent with the slightly larger coupling constants which we observed from Gaussian90 in the absence of solvent. Resorting to a higher basis set resulted in even higher theoretical coupling constants, since lower basis sets suffer from overly diffuse electronic field gradients (Ragle et al., 1974). Our hope was that the variation in the quadrupole coupling constants between sites realistically reflected the hydrogen bonding and local electronic environment, and that there was a simple systematic error in the overestimation of the coupling constants at the STO-3G* basis set level. This being the case, we could simply scale all coupling constants obtained from Gaussian90 by a constant factor such that e^2qQ/h = 167 kHz for the methyl deuteron on the Val side chain. Our analysis at the STO-3G* basis set level revealed a scaling factor of 0.925. To determine whether the theoretical quantum computational calculations of e^2qQ/h were sensitive to the presence of an adjacent hydrogen bond, some of the EFG calculations were performed (at different basis set levels) both in the presence and absence of the hydrogen bonded fragments. Some of these calculations are summarized in Table 1 which reveals several important features. Note that the calculated EFG asymmetry parameter (η) for the deuteron attached to the α-carbon atom is low, as is commonly observed in C—^{2}H systems (Vold and Vold, 1991). Furthermore, the NMR parameters (e^2qQ/h, η, ϕ_D, θ_D, and ψ_D) are reasonably consistent for a given fragment from one basis set to the next. Lastly, the calculations (even at the STO-3G* level) were clearly sensitive to the hydrogen bonding. In fact, for a given basis set, the quadrupolar coupling constants were observed to vary by nearly 40 kHz, as can be seen in Fig. 7, which graphs e^2qQ/h vs. $1/R^3$ for all fragments using an STO-3G* basis set. This variation in e^2qQ/h should be linearly related to the inverse cube of the distance (R) from the exchangeable deuteron to the hydrogen-bonded oxygen atom (Hunt and MacKay, 1974, 1976). Fig. 7 seems to exhibit this linear dependence; the solid line through the data points

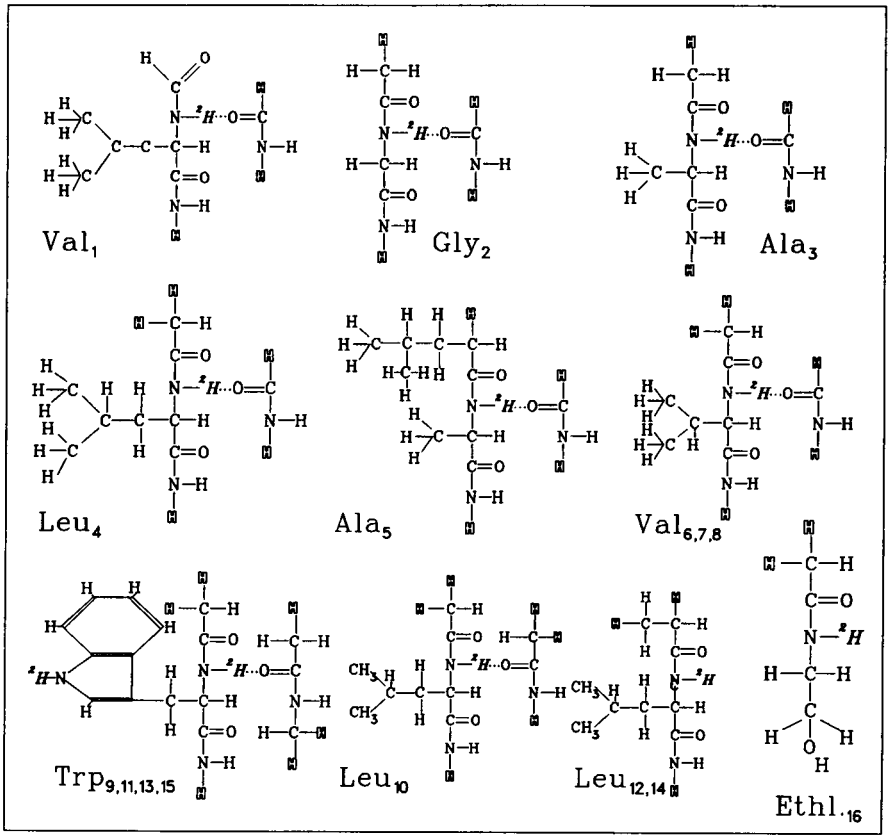

FIGURE 6 Molecular fragments analyzed by Gaussian90. Hydrogen bonds (···) and boundary atoms are also included. In this case a boundary atom is a hydrogen atom which replaces a carbon atom.

TABLE 1 Gaussian EFG parameters and corresponding ^{2}H NMR parameters derived for the "relaxed" Arseniev model

Residue and basis set	V_{xx}	V_{yy}	V_{zz}	V_{xy}	V_{xz}	V_{yz}	V_{aa}	V_{bb}	V_{cc}	e^2qQ/h	η	ϕ_D	θ_D	ψ_D
	H/B (a.u.)	H/B	H/B	H/B	H/B	H/B	H/B	H/B	H/B	kHz		°	°	°
Val_1 STO-3G*‡	0.1342	0.1225	−0.2568	−0.0051	0.0430	0.0763	0.1348	0.1413	−0.2761	180	0.023	293.2	12.4	299.1
Gly_2 STO-3G*§	0.1979	0.0007	−0.1986	−0.0198	0.0931	0.2709	0.1621	0.2383	−0.4004	261	0.190	311.1	35.2	284.6
Gly_2 6-31G*	0.1959	−0.0030	−0.1929	−0.0142	0.0985	0.2661	0.1506	0.2433	−0.3939	256	0.24	310.5	35.4	285.0
Gly_2 6-31G*§	0.2186	−0.0049	−0.2138	−0.0168	0.1030	0.2989	0.1726	0.2668	−0.4394	286	0.21	311.1	35.6	284.1
Gly_2 MP2/6-31G*§	0.1853	0.0010	−0.1863	−0.0163	−0.0919	0.2522	0.1472	0.2274	−0.3746	244	0.21	310.4	35.2	285.1

Rows two to five represent the theoretical EFG tensor (given in atomic units), and the corresponding NMR parameters, for an amide deuteron belonging to the Gly_2 residue of gramicidin. These numbers were derived from electron molecular orbital calculations using a program called Gaussian90 under various levels of approximation (represented by the basis sets, i.e., STO-3G*, 6-31G*, and MP2/6-31G*). The positions of the atoms were fixed according to the proposed "relaxed" Arseniev model structure.

‡ For comparison, row one depicts the EFG parameters for a deuteron bonded to the α-carbon atom of residue Val_1.

§ Calculations done in the absence of the hydrogen-bonded carboxyl fragment.

represents a least squares fit to the following relation:

$$\frac{e^2qQ}{h} = b - m/R^3 \qquad \text{kHz}, \tag{6}$$

where $b = 263.2 \pm 0.8$ kHz and $m = 234.0 \pm 1.0$ kHz Å^3. The other variable which one might expect to be related to the quadrupole coupling constant is the (N—H, C═O) bond angle. In the inset of Fig. 7, a histogram, which relates the occurrence of hydrogen-bond pairs to the (N—H, C═O) bond angle, has been included. In addition, we could find no simple correlation between the hydrogen bond angle and the quadrupole coupling constant.

As a further test of Gaussian90, we considered the EFG tensor of a methyl deuteron, and a deuteron directly bonded to an α-carbon atom, since in either case we expect the asymmetry parameter to be nearly zero and the Euler angle, θ_D to be virtually equal to the angle formed by the N—^{2}H bond and the helix axis. For deuterons attached directly to the C_α atom, our calculations at the STO-3G* level revealed that the EFG asymmetry parameter (η) was less than 0.025 with the principal axis of the EFG tensor within 0.5° of the bond (η was even closer to zero and θ_D correspondingly closer to the angle formed by the N—^{2}H bond and the helix axis for the methyl deuteron on the Val_1 side chain). For the amide deuterons, the calculated value of η was typically slightly less than 0.2 (0.14 for the indole groups) which is in agreement with lineshape simulations of Datema et al. (1986). In fact, all of our EFG calculations revealed the principal axis of the EFG tensor to be within 2.0° of the N—^{2}H bond. Thus, in the fast axially symmetric motional regime, it seems sufficient to employ a phenomenological equation to estimate the quadrupole coupling constant and to simply use the angles formed by the N—^{2}H bonds and the helix axis, in order to predict the spectrum. Nevertheless, the quadrupole coupling constant, the asymmetry parameter, and the complete set of Euler angles can be obtained from Gaussian90. These parameters would be potentially useful if one were to attempt to simulate spectra in a slower motional regime or if one were to simulate NMR relaxation studies. Furthermore, a deviation of 2.0° in θ_D translates into a difference of 1–2 kHz in an oriented spectrum, which is within the spectral resolution (particularly in a proton decoupled spectrum (Hing et al., 1990a, b). Thus, using Gaussian90, it is possible to proceed from a structural model to a theoretical spectrum, without the need to make assumptions about the EFG tensor. Perhaps the most important result obtained from Gaussian90 is the small deviation of the principal axis of the EFG tensor from the N—^{2}H bond.

Lastly, we must ask if the STO-3G* basis is sufficient to represent the EFG tensor at the nucleus. Although the Gaussian90 calculations yielded reasonable fast motional limit spectra, asymmetry parameters, and quadrupole coupling constants, we can not be sure that the basis sets which we have used are sufficient to accurately portray the EFG tensor of interest. For the Gly_2 fragment, both SCF calculations at the STO-3G* and 6-31G* basis set levels, gave similar EFG tensors. As a final check on the reliability of our basis set we employed an MP2/6-31G basis set, in which actual electron-electron correlation was treated (as opposed to the SCF level where electron correlation is not explicitly considered) to calculate the EFG tensor for the amide deuteron of the Gly_2 fragment (Fig. 7). Again, the resulting EFG tensor and corresponding Euler angles were found to be similar to those calculated at the SCF level (Prosser, 1992).

Accounting for the motional narrowing:

Although the simulated spectra from Fig. 5 resembled the experimental spectra in shape, the model-based splittings were generally slightly higher than their experimental counterparts. If we assume the peptide backbone to be rigid and imagine the peptide to undergo only diffusion around the helix axis, then we would expect no additional motional narrowing. We therefore hypothesize that the additional motional narrowing is due primarily to another whole body motion—diffusion of the peptide around its minor axis, perpendicular to the helix axis (or more precisely, wobble of the peptide within a Maier-Saupe orienting potential (Cotter, 1977)).[2] Molecular motion

[2] We will discuss details of these motions in a subsequent paper.

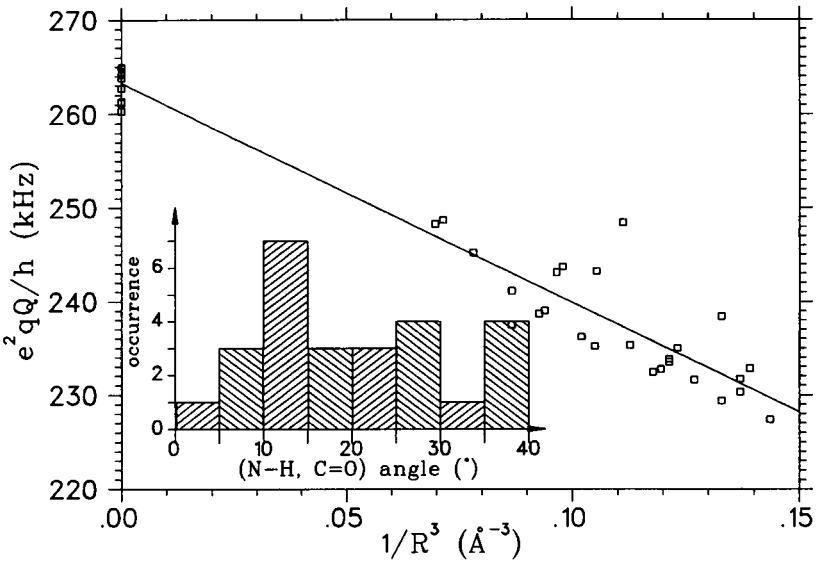

FIGURE 7 e^2qQ/h vs. $1/R^3$ for exchangeable deuterons in GD fragments from Gaussian90 calculations using an STO-3G* basis set. R represents the distance from the exchangeable deuteron to the hydrogen-bonded oxygen atom. Inset: histogram displaying the frequency of fragments having a particular (N—H, C═O) bond angle.

will thus modulate the Euler angles so that the splitting, $\Delta\nu_Q$, is determined by an average over these orientations (this was alluded to by the *bar* over part of the expression for $\Delta\nu_Q$ in Eq. 1). In this case, $\langle\theta^2\rangle \neq 0$ (see Eq. 1) and the quantity $\overline{(1/2)(3\cos^2\theta - 1)}$ is a molecular order parameter which scales all of the splittings of the "rigid" molecule by the same factor. Knowledge of the quadrupole coupling constant and θ_D permits us to estimate the "molecular" order parameter. In fact, we can speculate that the motional narrowing implicit in the molecular order parameter is due to motions such as "wobbling" diffusion of the peptide in the membrane (Mayer et al., 1988, 1990), lateral diffusion over curvature defects in the multilayers (Bloom et al., 1992), director fluctuations (Stohrer et al., 1991), and/or surface undulations (Bloom and Evans, 1990). Furthermore, if we assumed that these motions were uncorrelated, we could separate the narrowing contributions to the molecular order parameter due to the above motions as follows:

$$S_{mol} = S_{ZZ}S_{LD}S_{ODF}, \tag{7}$$

where S_{ZZ}, S_{LD}, and S_{ODF} are parameters describing the ordering due to libration (or wobble), lateral diffusion, and order director fluctuations, respectively. For oriented samples, we assume that the contribution to narrowing due to lateral diffusion over curvature defects, is negligible. In addition we make use of the experimental result of Stohrer et al. (1991) who estimate that $S_{ODF} \approx 0.97$ for a similar system. Therefore from Eq. 6, we can calculate the molecular order parameter due only to whole body wobbling diffusion. Now returning to Fig. 5 *c*, we can extract the theoretical splittings of the outermost doublets corresponding to residues 1, 5, 7, and 9 and by comparing with the observed outermost quadrupolar splitting (= 137.4 kHz) solve for the order parameter, which yields $S_{mol} = 0.857$. After correcting for possible order director fluctuations, we obtain a molecular order parameter, $S_{ZZ} = 0.884$.

Until now, we have assumed that gramicidin A is rigid, when in fact there is at least one significant intramolecular motional mechanism which may have an effect on the motional narrowing of amide deuterons—helical librations, as discussed by Venkatachalam and Urry (1983, 1984) and others (Nicholson et al., 1991; North and Cross, 1993; Roux and Karplus, 1988, 1991; Teng et al., 1991). Urry explains this motion as a crankshaft mechanism in which the orientation of a given peptide plane is changed without appreciably altering the positions of the rest of the atoms of the molecule. For a given dipeptide in the helix, whose backbone structure may be described by the standard torsional angles $\{\psi_i, \phi_i, \psi_{i+1}, \phi_{i+1}\}$, the peptide plane, formed by the carboxyl and amide groups, can librate via a change in the torsional angle ψ_i and an equal but opposite change in ϕ_{i+1}, without significant movement of the rest of the peptide. More recent work by Roux and Karplus (1988, 1991) using a normal mode analysis, suggests that the characteristic time scales of these helical librations are between 1.2 and 2.8 $\times 10^{-12}$ s. If the motion is fast compared to the quadrupole coupling constant (as is the case here) then we can build in the effect on the motional narrowing (see Eq. 1) by considering the average, $(1/2)\overline{(3\cos^2\theta_D - 1)}$. Roux and Karplus (1988) further determined that the root mean square angular deviation of the amide groups was approximately 12.5°, and that this was somewhat uniform throughout the peptide, with the exception of the amide group in Val_6 whose rms deviation was closer to 28°. Assuming a simple Gaussian distribution in the angular deviation (δ) of the torsional angle from its equilibrium value,

$$f(\delta) = \frac{1}{\sqrt{\pi\sigma}}e^{-\delta^2/\sigma^2}, \tag{8}$$

we could estimate the average value of $(1/2)(3\cos^2\theta_D - 1)$. This was done by constructing a model of the Ala_3Leu_4 dipeptide whose atomic coordinates came from a right-handed $\beta_{LD}^{6,3}$ helical model. An ensemble of 23 helically librated conformers of this dipeptide was constructed in which ψ_3 and ϕ_4 were incrementally varied by $\pm 3°$ and $\mp 3°$ from their respective equilibrium values. Each conformer was assigned a probability according to the magnitude of deviation, δ, of the torsional angles (ψ_3 and ϕ_4) from their equilibrium values (i.e., the probability of conformer i is given by $p(i) = Ne^{-\delta_i^2/\sigma^2}$ where δ_i is the angular deviation of the ith conformer and N is a normalization factor). The weighted average of $(1/2)(3\cos^2(\theta_D) - 1)$ for the amide bond of Leu_4 was then calculated. Assuming $\sigma = 12.5°$ (Roux and Karplus, 1988), this average was calculated to be 0.843 (compared to $(1/2)(3\cos^2(\theta_D) - 1) = 0.867$ for a constant value of $\theta_D = 162.7°$). This yields a motional narrowing factor of 0.972, which we would also expect for all of the amides except for that from Val_6 (Roux and Karplus, 1988). We also considered 23 helically librated conformers of the Ala_5Val_6 dipeptide, in which ψ_3 and ϕ_4 were incrementally varied by $\pm 6°$ and $\mp 6°$ from their equilibrium values, assuming $\sigma = 28°$. In this case, the weighted ensemble average of $(1/2)(3\cos^2(\theta_D) - 1)$ was calculated to be 0.596 (compared to $(1/2)(3\cos^2(\theta_D) - 1) = 0.707$ for $\theta_D = 153.8°$); the corresponding motional narrowing factor for this particular amide deuteron is then 0.843. Thus, if we account for the motional narrowing due to helical libration, we obtain a new estimate for the molecular order parameter due to librational diffusion ($S_{ZZ} = 0.91$) in which case the rms average angle becomes approximately 14°. This result appears to be in agreement with the findings of Separovic et al. (1993) who estimate the overall molecular order parameter to be 0.93 ± 0.03. This molecular order parameter may also be compared with that of Taylor et al. (1981) in which the molecular order parameter of cholesterol in unoriented DMPC multilamellar dispersions was

determined to be 0.87. Our assumption that gramicidin was a rigid molecule means that any motional narrowing is uniform to all residues; the calculations of Roux and Karplus (1988, 1991) suggest that, despite the fact that gramicidin is not strictly rigid, the motional narrowing due to intramolecular helical librations is roughly constant, except for the amide group belonging to Val_6. Thus, if we were to account for this intramolecular motion in the theoretical spectra, we might wish to reduce the splitting corresponding to Val_6 by 0.843/0.972 (= 0.867). Roux and Karplus (1988) have hypothesized that the apparent additional mobility of the C, O, N, H peptide plane (from Ala_5Val_6) may be due to the fact that it is hydrogen-bonded to the flexible formyl group of the opposite monomer. We have not considered the potential additional motional narrowing of the Trp indole groups due to rapid (Macdonald and Seelig, 1988) dihedral angle fluctuations. The normal mode analysis by Roux and Karplus (1988) suggests that the rms side-chain dihedral angle fluctuations (χ_1 and χ_2) are ~10°, although the fluctuation in χ_1 is significantly larger for Trp_0 and Trp_{15} (~20°). In principle, we could consider the (weighted) ensemble of orientations of each of the indole N—^{2}H groups, just as we did with the amide Val_6 group, in order to determine the additional motional narrowing of each indole moiety. However, the Trp side-chain conformational substrates are less well known, both theoretically and experimentally. Thus, the splittings for the indole moieties in the theoretical spectra presented above should be considered as upper limits. The ethanolamine group may also undergo additional reorientations (Etchebest and Pullman, 1986) as it facilitates cation transport.

In Fig. 8, the oriented spectrum of GD in the fast motionally symmetric regime is simulated from the "relaxed" Arseniev model (Killian et al., 1992) incorporating the Euler angles (θ_D obtained from the work with Gaussian90, and considering the intramolecular motional narrowing of the Val_6 residue. Note that the spectrum in Fig. 8 is very similar to that shown in Fig. 5 *c*.

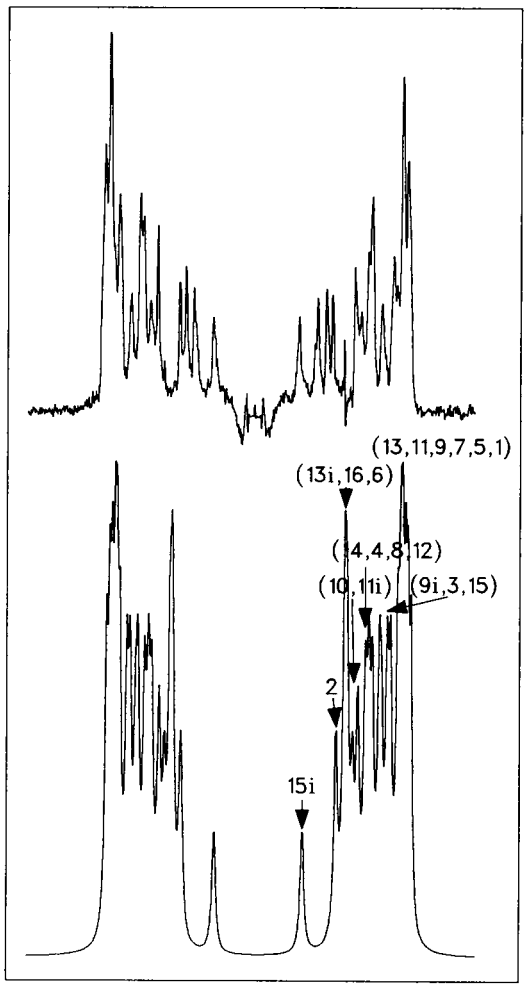

FIGURE 8 Theoretical fast motional limit ^{2}H NMR spectrum of oriented exchange-labeled GD, derived from the right-handed "relaxed" Arseniev model. The spectrum has been calculated without considering the effects of hydrogen bonding. In this case the Euler angles, θ_D, from the Gaussian90 calculations (using an STO-3G* basis set) have been used in calculating the splittings. The presumed motional narrowing attributed to the Val_6 residue has also been incorporated. The peaks have been labeled according to the residue from which they originate; a suffix "i" after the residue number indicates the indole moiety (otherwise the number(s) assigned to a given peak indicate(s) the residue number of the amide moiety).

CONCLUSIONS

In this paper we have described how we used ^{2}H NMR spectroscopy on exchange-labeled gramicidin D to study the dynamic structure of the peptide in oriented DLPC multilayers. The resulting spectra showed no observable powder fractions and resembled the dePaked spectra of the same labeled molecule in DPPC multilayers (Datema et al., 1986). Our results were also similar to those of Davis (1988) who studied exchange labeled GD in an oriented lyotropic nematic phase (at θ_{or} = 90°). This suggests that the orientational order of integral membrane peptides such as gramicidin in the lyotropic nematic phase is similar to that of the lipid bilayer.

There are numerous complications associated with interpreting ^{2}H NMR spectra from exchangeable deuterons in a transmembrane peptide. First, hydrogen bonding causes the quadrupole coupling constant to decrease (by as much as 40 kHz in our case). This effect can either be accounted for phenomenologically (Hunt and MacKay, 1974, 1976) or quantum mechanically, using an ab initio program called Gaussian90 (Frisch et al., 1990). The second complication is the asymmetry parameter associated with the EFG tensor, which for deuterons bonded to nitrogen atoms is typically 0.2. Using Gaussian90, it is also possible to determine the Euler angles involved in the transformation of the EFG tensor from its PAS to the molecular diffusion tensor system (i.e., rather than use the bond angle in the expression for the quadrupolar splitting, we can use the Euler angle, which is appropriate when η is nonzero). We also performed several quantum computational calculations on the Gly_1 residue to determine the EFG tensor, both including and excluding the hydrogen-bonded fragment, and using two SCF basis sets (STO-3G* and 6-31G*) and an MP2/6-31G basis set, which partly accounts for electron correlations. In all cases, the EFG parameters were similar. We have attempted to assess the reliability of the Gaussian90 calculations on the basis of comparison of calculated asymmetry parameters with lineshape simulations (Datema, 1986), the variation of the quadrupole coupling constant with hydrogen bond lengths (and the corresponding experimental results (Hunt and MacKay, 1974, 1976)), and the similarity between experimental and theoretical quadrupolar splittings. Nevertheless, the results of Gaussian90 are only as good as the model from which the atomic coordinates were obtained.

Using any level of approximation, the oriented spectra are completely inconsistent with any of the left-handed models we considered. The right-handed models (particularly the models based on Arseniev's structure) yielded theoretical spectra with many features in common with our experimental spectra. In particular, the right-handed "relaxed" Arseniev model (Killian et al., 1992) yielded a spectrum that was similar to the observed spectrum. When the effects of hydrogen bonding were incorporated into our spectra (recall that hydrogen bonding is expected to decrease the quadrupole coupling constant), the agreement was not as good. We proposed that the non-hydrogen-bonded fragments, which are known to exist in the outer turn of the peptide helix, undergo additional intramolecular motional narrowing and narrowing through exchange and dynamic hydrogen bonding with water molecules. Future Langevin molecular dynamics simulations (B. Roux and J. Davis, personal communication) of the peptide should permit us to incorporate these exchange effects into our simulated spectra.

Finally, we discussed motional narrowing effects arising from whole body and intramolecular motions. After considering narrowing effects due to intramolecular helical libration, we arrived at a molecular order parameter of 0.88 due to whole body motions. Accounting for the possibility of order director fluctuations, we were able to estimate the molecular order parameter due to "wobble" of the peptide in an Maier-Saupe restoring potential. The resulting order parameter was $S_{ZZ} = 0.91$, which translates into an rms angle of approximately 14°.

FUTURE PROSPECTS

Although gramicidin is a small hydrophobic peptide which is easily incorporated into membranes, it should be possible to extend the methods described in this paper to study the dynamic structure of other membrane peptides and proteins. As long as the correlation time(s) is (are) not in the vicinity of $(e^2qQ/h)^{-1}$, then the signal to noise ratio should be sufficient to obtain reasonable spectra. Studies of GA oriented in perdeuterated DLPC indicated we could obtain oriented spectra (with no observable powder fraction) even if we increased the amount of sample per plate by 50% and reduced the ratio of lipid to peptide from 15:1 to 10:1. By proton decoupling (Hing et al., 1990a,b) Hing and coworkers have been able to reduce the effective T_{2E} by a factor of two. Other labs have also experimented with ultra-thin plates in which the plate thickness was 0.025 mm, rather than the standard 0.1-mm thickness (T. M. Bayerl, personal communication); since conventional glass plates typically occupy half the usable sample volume, such ultra-thin plates would result in a 100% increase in sample content. These changes alone would result in nearly a 5-fold improvement in *S/N*. Higher field strengths would also improve *S/N*. For example: using a 500-MHz (^{1}H Larmor frequency) field strength instead of a 360-MHz field would result in an improvement in *S/N* by a factor of 1.6. For smaller peptides, T_{2E} in the lyotropic nematic liquid crystalline host Davis (1988) appears to be significantly longer than in the oriented lipid multilayer system. Thus, there appears to be significant room for detailed spectroscopic and NMR relaxation studies of other membrane peptide and protein systems by ^{2}H NMR.

Because GD consists of 20 separate labels, assignment is difficult, except from model structures which are very close to the experimental structure. Nevertheless, by specific ^{15}N labeling, all of the doublets could be assigned. One strategy would be to perform a double resonance experiment wherein the labeled ^{15}N spin was alternately inverted by a π pulse and left alone, immediately before performing a quadrupole echo sequence on the deuterated system. The difference of the two FIDs would yield a doublet(s), for the deuteron(s) adjacent (i.e., directly bonded) to the ^{15}N label. We must also acknowledge that we did not study gramicidin A but rather gramicidin D, whose first and eleventh residues consist partially of a mixture of residues, as discussed earlier. The exchange labeled spectrum of a single species, gramicidin A, should be measured. In addition, proton decoupling should be employed as we could then expect to see nearly a twofold gain in resolution (Hing et al., 1990a,b).

In this paper, we have argued that it is possible to start with a three-dimensional model and simulate an oriented spectrum which accurately reflects the structural details of the model. As models improve in accuracy, quantum computational calculations will become important in assessing the validity of the model structure. We have also stressed that an exchange-labeled spectrum contains a wealth of structural information, without the need for isotopic labeling. We propose that, since much of the structural information in the spectrum has been sorted out, such exchange-labeled spectra could be obtained under various conditions (e.g., ion concentration or pH, lipid composition, etc.) in order to explore lipid-protein interactions and the connection between structure and function.

Many thanks to R. A. Kirby who performed the MP2/6-31G calculations at the Southern Illinois University Computing Center, to Prof. Mike Morrow at Memorial University, Newfoundland, for helpful comments, and to Denis Langlais for assistance in preparing this manuscript.

This work was supported by grants from the Natural Sciences and Engineering Research Council of Canada.

REFERENCES

Åqvist, J. 1986. A simple way to calculate the axis of an alpha-helix. *Computers and Chem.* 10:97–99.

Arseniev, A. S., I. L. Barsukov, V. F. Bystrov, A. L. Lomize, and Y. A. Ovchinnikov. 1985. ^{1}H-NMR study of gramicidin A transmembrane ion channel. *FEBS Lett.* 186:168–174.

Arseniev, A. S., A. L. Lomize, I. L. Barsukov, and V. F. Bystrov. 1986. Gramicidin A transmembrane channel three-dimensional structure reconstruction based on NMR spectroscopy and conformational energy refinement. *Biol. Membr.* 3:1077–1104.

Bāno, M. C., L. Braco, and C. Abad. 1991. Conformational transitions of gramicidin A in phospholipid model membranes. A high-performance liquid chromatography assessment. *Biochemistry.* 30:886–894.

Bloom, M., J. H. Davis, and M. I. Valic. 1980. Spectral distortion effects due to finite pulse widths in deuterium NMR spectroscopy. *Can. J. Phys.* 58:1510–1517.

Bloom, M., and E. Evans. 1990. Observations of surface undulations on the mesoscopic length scale by NMR. *In* NATO Adv. Workshop for Biologically Inspired Physics. Pelliti, L., editor. Plenum Press, New York. 137–147.

Bloom, M., C. Morrison, E. Sternin, and J. L. Thewalt. 1992. Spin echoes and the dynamic properties of membranes. *In* Pulsed Magnetic Resonance: NMR, ESR, and Optics, a Recognition of E. L. Hahn. Bagguley, D. M. S., editor. Clarendon Press, Oxford. 274–316.

Bystrov, V. F., and A. S. Arseniev. 1988. Diversity of the gramicidin A spatial structure: Two-dimensional proton NMR study in solution. *Tetrahedron*. 44:925–940.

Chiu, S., L. Nicholson, M. Brenneman, S. Subramanian, Q. Teng, C. North, J. McCammon, T. Cross, and E. Jakobsson. 1990. Molecular dynamics computations and solid state NMR of the gramicidin cation channel. *Biophys. J.* 57:101a.

Cotter, M. A. 1977. Hard spherocylinders in an anisotropic mean field: A simple model for a nematic liquid crystal. *J. Chem. Phys.* 66:1098–1106.

Cox, K. J., C. Ho, J. V. Lombardi, and C. D. Stubbs. 1992. Gramicidin Conformational Studies with Mixed-Chain Unsaturated Phospholipid Bilayer Systems. *Biochemistry*. 31:1112–1118.

Datema, K. P., K. P. Pauls, and M. Bloom. 1986. Deuterium NMR investigation of the exchangeable sites on gramicidin A and gramicidin S in multilamellar vesicles of dipalmitoylphosphatidylcholine. *Biochemistry*. 25:3796–3803.

Davis, J. H. 1979. Deuterium Magnetic Resonance Study of the Gel and Liquid Crystalline Phases of Dipalmitoyl Phosphatidylcholine. *Biophys. J.* 27:339–358.

Davis, J. H. 1983. The description of membrane lipid conformation, order and dynamics by ^{2}H-NMR. *Biochim. Biophys. Acta*. 737:117–171.

Davis, J. H. 1988. ^{2}H NMR of exchange-labeled gramicidin in an oriented lyotropic nematic phase. *Biochemistry*. 27:428–436.

Davis, J. H. 1993. The molecular dynamics, orientational order and thermodynamic phase equilibria of cholesterol/phosphatidylcholine mixtures: ^{2}H NMR. *In* Cholesterol in Membrane Models. L. Finegold, editor. CRC Press, Boca Raton, Florida. 67–136.

Davis, J. H., K. R. Jeffrey, M. Bloom, M. I. Valic, and T. P. Higgs. 1976. Quadrupolar echo deuteron magnetic resonance spectroscopy in ordered hydrocarbon chains. *Chem. Phys. Lett.* 42:390–394.

Deisenhofer, J., and H. Michel. 1989. The Photosynthetic Reaction Center from the Purple Bacterium Rhodopseudomonas viridis. *Science*. 245:1463–1473.

Etchebest, C., and A. Pullman. 1986. The gramicidin A channel. *FEBS Lett.* 204:261–265.

Fields, C. G., G. G. Fields, R. L. Noble, and T. A. Cross. 1989. Solid phase peptide synthesis of ^{15}N-gramicidins A, B, and C and high performance liquid chromatographic purification. *Int. J. Pept. Protein Res.* 33: 298–303.

Frisch, M. J., M. Head-Gordon, G. W. Trucks, J. B. Foresman, H. B. Schlegel, K. Raghavachari, M. Robb, J. S. Binkley, C. Gonzalez, D. J. Defrees, D. J. Fox, R. A. Whiteside, R. Seeger, C. F. Melius, J. Baker, R. L. Martin, L. R. Kahn, J. J. P. Stewart, S. Topiol, and J. A. Pople. 1990. GAUSSIAN 90, Revision F, GAUSSIAN, INC., Pittsburgh, PA, USA.

Gennis, R. B. 1989. *Biomembranes: Molecular Structure and Function*, Springer-Verlag, New York.

Greathouse, D. V., and R. E. Koeppe II. 1992. Gramicidin A dispersions in short-chain phospholipids: Effect of lipid chain length on gramicidin conformation. *Biophys. J.* 61:A526.

He, K., Ludtke, J., Yili Wu, and H. W. Huang. 1993. X-ray scattering with momentum transfer in the plane of the membrane. *Biophys. J.* 64: 157–162.

Heaton, N. J., R. R. Vold, and R. L. Vold. 1988. Deuterium quadrupole-echo NMR spectroscopy. IV. Inversion of full width deuterium powder patterns. *J. Magn. Res.* 77:572–576.

Henderson, R., J. M. Baldwin, T. A. Ceska, F. Zemlin, E. Beckmann, and K. H. Downing. 1990. Model for the structure of bacteriorhodopsin based on high-resolution electron cryo-microscopy. *J. Mol. Biol.* 213:899–929.

Hinchliffe, A. 1987. *Ab Initio Determination of Molecular Properties*, Adam Hilger, Bristol.

Hing, A. W., S. P. Adams, D. F. Silbert, and R. E. Norberg. 1990a. Deuterium NMR of Val^1···(2-^{2}H)Ala^3···gramicidin A in oriented DMPC bilayers. *Biochemistry*. 29:4144–4156.

Hing, A. W., S. P. Adams, D. F. Silbert, and R. E. Norberg. 1990b. Deuterium NMR of ^{2}HCO-Val^1···gramicidin A and ^{2}HCO-Val^1-D-Leu^2···gramicidin A in oriented DMPC bilayers. *Biochemistry*. 29: 4156–4166.

Hunt, M. J., and A. L. Mackay. 1974. Deuterium and nitrogen pure quadrupole resonances in deuterated amino acids. I. *J. Magn. Res.* 15: 402–414.

Hunt, M. J., and A. L. Mackay. 1976. Deuterium and nitrogen pure quadrupole resonance in amino acids. II. *J. Magn. Res.*22:295–301.

Katsaras J., R. H. Stinson, and J. H. Davis, 1994, x ray diffraction studies of oriented phosphatidylcholine bilayers in the L_δ and L_α phases. *Acta Cryst. Sect. B.* 50:208–216.

Killian, J. A., K. U. Prasad, D. Hains, and D. W. Urry. 1988. The membrane as an environment of minimal interconversion. A circular dichroism study on the solvent dependence of the conformational behavior of gramicidin in diacylphosphatidylcholine model membranes. *Biochemistry*. 27:4848–4855.

Killian, J. A. 1992. Gramicidin and gramicidin-lipid interactions. *Biochim. Biophys. Acta*. 1113:391–425.

Killian, J. A., M. J. Taylor, and R. E. Koeppe II. 1992. Orientation of the valine-1 side chain of the gramicidin transmembrane channel and implications for channel functioning. A ^{2}H NMR study. *Biochemistry*. 31: 11283–11290.

LoGrasso, P., F. Moll, and T. A. Cross. 1988. Solvent History of Gramicidin A Conformations in Hydrated Lipid Bilayers. *Biophys. J.* 54:259–267.

Macdonald, P. M., and J. Seelig. 1988. Dynamic properties of gramicidin A in phospholipid membranes. *Biochemistry*. 27:2357–2364.

Mayer, C., G. Gröbner, K. Müller, K. Weisz, and G. Kothe. 1990. Orientation-dependent spin-lattice relaxation times in bilayer membranes: characterization of the overall lipid motion. *Chem. Phys. Lett.* 165:155–161.

Mayer, C., K. Müller, K. Weisz, and G. Kothe. 1988. Deuteron NMR relaxation studies of phospholipid membranes. *Liquid Cryst.* 3:797–806.

Meier, P., E. Ohmes, and G. Kothe. 1986. Multipulse dynamic NMR of phospholipid membranes. *J. Chem. Phys.* 85:3598–3614.

Moll, F., and T. A. Cross. 1990. Optimizing and characterizing alignment of oriented lipid bilayers containing gramicidin D. *Biophys. J.* 57: 351–362.

Morrow, M. R. 1990. Transverse nuclear spin relaxation in phosphatidyl choline bilayers containing gramicidin. *Biochim. Biophys. Acta*. 1023: 197–205.

Morrow, M. R., and J. H. Davis. 1987. Calorimetric and NMR study of the phase behavior of dilauroylphosphatidylcholine/water. *Biochim. Biophys. Acta*. 904:61–70.

Morrow, M. R., and J. H. Davis. 1988. Differential scanning calorimetry and ^{2}H NMR studies of the phase behavior of gramicidin-phosphatidylcholine mixtures. *Biochemistry*. 27:2024–2032.

Morrow, M., G. A. Simatos, R. Srinivasan, N. Grandal, L. Taylor, and K. M. W. Keough. 1991. The effect of changes in gramicidin conformation on bilayer lipid properties. *Biochim. Biophys. Acta*. 1070:209–214.

Nicholson, L. K., Q. Teng, and T. A. Cross. 1991. Solid-state nuclear magnetic resonance derived model for dynamics in the polypeptide backbone of the gramicidin A channel. *J. Mol. Biol.* 218:621–637.

North, C. L., and T. A. Cross. 1993. Analysis of polypeptide backbone T_1 relaxation data using an experimentally derived model. *J. Magn. Res.* (in press).

Opella, S. J., P. L. Stewart, and K. G. Valentine. 1987. Protein structure by solid-state NMR spectroscopy. *Q. Rev. Biophys.* 19:7–49.

Opella, S. J., and P. L. Taylor. 1989. In *Methods Enzymol.*, Oppenheimer, N. J., and James, J. L., Eds., 176:242–275, Academic Press, Toronto.

Prosser, R. S. 1992. The structure and dynamics of an amphiphilic peptide: A deuterium NMR relaxation study of gramicidin A. PhD Thesis. University of Guelph.

Prosser, R. S., J. H. Davis, F. W. Dahlquist, and M. A. Lindorfer. 1991. ^{2}H NMR of the gramicidin A backbone in a phospholipid bilayer. *Biochemistry*. 30:4687–4696.

Prosser, R. S., J. H. Davis, C. Mayer, K. Weisz, and G. Kothe. 1992. Deuterium NMR relaxation studies of peptide-lipid interactions. *Biochemistry*. 31:9355–9363.

Prosser, R. S., and J. H. Davis. 1994. Structural dynamics of an integral

membrane peptide: A deuterium NMR relaxation study. *Biophys. J.* 66: 1429–1440.

Ragle, J. L., G. Minott, and M. Mokarram. 1974. Deuterium quadrupole coupling in solid complexes of diethyl ether, acetone, and mesitylene with chloroform-d. *J. Chem. Phys.* 60:3184–3194.

Rice, D., and E. Oldfield. 1979. Deuterium NMR studies of the interaction between dimyristoylphosphatidylcholine and gramicidin A'. *Biochemistry.* 18:3272–3279.

Roux, B., and M. Karplus. 1988. The normal modes of the gramicidin-A dimer channel. *Biophys. J.* 53:297–309.

Roux, B., and M. Karplus. 1991. Ion transport in a gramicidin-like channel: Dynamics and mobility. *J. Phys. Chem.* 95:4856–4868.

Sarges, R., and B. Witkop. 1965. Gramicidin. VIII. The structure of Valine- and Isoleucine-gramicidin C. *Biochemistry.* 4:2491–2494.

Separovic, F., R. Pax, and B. Cornell. 1993. NMR order parameter analysis of a peptide plane in a lyotropic liquid crystal. *Mol. Phys.* 78:357–369.

Simons, J. 1991. The experimental chemist's guide to ab initio quantum chemistry. *J. Phys. Chem.* 95:1017–1029.

Smith, R., D. E. Thomas, F. Separovic, A. R. Atkins, and B. A. Cornell. 1989. Determination of the structure of a membrane-incorporated ion channel. *Biophys. J.* 56:307–314.

Stankovic, C., J. Delfino, and S. Schreiber. 1990. Purification of gramicidin A. *Anal. Biochem.* 184:100–103.

Stohrer, J., G. Gröbner, D. Reimer, K. Weisz, C. Mayer, and G. Kothe. 1991. Collective lipid motions in bilayer membranes studied by transverse deuteron spin relaxation. *J. Chem. Phys.* 95:672–678.

Szabo, A., and N. S. Ostlund. 1982. *Modern Quantum Chemistry: Introduction to Advanced Electronic Structure Theory*, Macmillan Publishing, New York.

Taylor, M. G., T. Akiyama, H. Saito, and I. C. P. Smith. 1981. Direct observation of the properties of cholesterol in membranes by deuterium NMR. *Chem. Phys. Lipids.* 29:327–339.

Teng, Q., L. K. Nicholson, and T. A. Cross. 1991. Experimental determination of torsion angles in the polypeptide backbone of the gramicidin A channel by solid state nuclear magnetic resonance. *J. Mol. Biol.* 218: 607–619.

Venkatachalam, C. M., and D. W. Urry. 1983. Theoretical and conformational analysis of the gramicidin A transmembrane channel. I. Helix sense and energetics of head-to-head dimerization. *J. Comput. Chem.* 4:461–469.

Venkatachalam, C. M., and D. W. Urry. 1984. Theoretical analysis of the gramicidin A transmembrane channel. II. Energetics of helical librational states of the channel. *J. Comput. Chem.* 5:64–71.

Vold, R. R., and R. L. Vold. 1991. Deuterium relaxation in molecular solids. *In* Advances in Magnetic and Optical Resonance, Vol. 16, pp. 85–171, Warren, W., Ed., Academic Press, New York.

Wallace, B. A. 1992. Crystallographic studies of a transmembrane ion channel, gramicidin A. *Biophys. Molec. Biol.* 57:59–69.

Wallace, B. A., and R. W. Janes. 1991. *J. Mol. Biol.* 217:625–627.

Wüthrich, K. 1986. *NMR of Proteins and Nucleic Acids*, John Wiley and Sons Inc., New York.